

1 **Cloud condensation Nuclei over the Southern Ocean: wind** 2 **dependence and seasonal cycles**

3 John L. Gras¹ and Melita Keywood¹

4 ¹Oceans and Atmosphere, CSIRO, Aspendale, 3195, Australia

5 *Correspondence to:* Melita Keywood (melita.keywood@csiro.au)

6 **Abstract.** Multi-decadal observations of aerosol microphysical properties from regionally representative sites can be used to
7 challenge regional or global numerical models that simulate atmospheric aerosol. Presented here is an analysis of multi-decadal
8 observations at Cape Grim (Australia) that characterise production and removal of the background marine aerosol in Southern
9 Ocean marine boundary layer (MBL) on both short-term weather-related and underlying seasonal scales.

10 A trimodal aerosol distribution comprises Aitken nuclei (< 100 nm), CCN/accumulation (100-350 nm) and coarse mode
11 particle (> 350 nm) modes, with the Aitken mode dominating number concentration. While the integrated particle number in
12 the MBL over the clean Southern Ocean is only weakly dependent on wind speed the different modes in the aerosol size
13 distribution vary in their relationship with wind speed. The balance between a positive wind dependence in the coarse mode
14 and negative dependence in the accumulation/CCN mode leads to a relatively flat wind dependence in summer and moderately
15 strong positive wind dependence in winter. The change-over in wind dependence of these two modes occurs in a very small
16 size range at the mode intersection, indicative of differences in the balance of production and removal in the coarse and
17 accumulation/CCN modes.

18 While a marine biological source of reduced sulfur appears to dominate CCN concentration over the summer months
19 (December to February) other components contribute to CCN over the full annual cycle. Wind-generated coarse mode sea-
20 salt is an important CCN component year round and is the second most important contributor to CCN from autumn through to
21 mid-spring (March to November). A portion of the non-seasonal dependent contributor to CCN can clearly be attributed to
22 wind generated sea-salt with the remaining part potentially being attributed to long range transported material. Under
23 conditions of greater supersaturation, as expected in more convective cyclonic systems and their associated fronts, Aitken
24 mode particles become increasingly important as CCN.

25 **1 Introduction**

26 There can be little doubt that global numerical models that include realistic aerosol microphysical processes, coupled with
27 accurate data on aerosol and precursors are the best tools to understand future aerosol impacts on climate, as attested by
28 developments such as Spracklen et al. (2005), Pierce et al. (2006), Korhonen et al. (2008), Wang et al. 2009, Mann et al.
29 (2010) and Lee et al. (2015). While one significant component in the building of confidence in such models is the availability

30 of representative climatologies of aerosol properties, such as cloud condensation nucleus (CCN) concentration on a global
31 scale, information on the range of aerosol properties on this scale, certainly from in-situ observations, is always likely to be
32 relatively limited. Multi-decadal observations of a wider range of properties from regionally-representative sites provide a
33 complementary basis for challenging these models, including for example dependencies on meteorology, seasonal and inter-
34 annual variations. With continuing refinement of microphysical representations within climate models there are opportunities
35 to examine these more subtle features of the aerosol within its very dynamic relationship in the weather-climate system as
36 well as refine the understanding of the various sources that contribute to aerosol regionally.

37 Work reported here draws on multi-decadal observations at Cape Grim (Australia) to characterise aspects of the clean marine
38 aerosol related to production and removal in the Southern Ocean marine boundary layer (MBL) on two different timescales.
39 The first is short-term weather-related and the second is a re-examination of underlying seasonal-scale variations. Particles
40 examined include two broad populations, Aitken nuclei and CCN. Aitken nuclei are represented by N3 and N11, where N3 is
41 the concentration integrated across all particle diameters greater than 3 nm and N11 likewise for particle diameters greater
42 than 11 nm (for these observations there is a practical upper size limit of 10 μm). This population is usually dominated by
43 particles in the Aitken mode, which in this MBL has a number distribution mode diameter around 20 nm. CCN is the
44 population of particles active at supersaturation levels typical of clouds; for this work the population examined mainly
45 comprises particles active at a supersaturation of 0.5% (CCN0.5) and at 0.23% (CCN0.23); the calculated lower particle size
46 threshold is composition dependent but typically for CCN0.5 includes particles larger than approximately 50 nm diameter and
47 for 0.23% around 78 nm. These particles comprise a significant fraction of the MBL accumulation or cloud-processed mode.

48 One very characteristic feature of aerosol in the Southern Ocean MBL is a strong and persistent underlying seasonal cycle that
49 in many aspects resembles a seasonal “pulse” over the summer months (December, January and February). This underlying
50 pattern of seasonal variation was used for example by Bigg et al. (1984), as evidence linking MBL N3 particle population to
51 solar radiation and a probable free troposphere source. Seasonal covariance of aerosol and methane sulfonic acid (MSA), an
52 aerosol phase oxidation product of dimethyl sulphide (DMS) was also used by Ayers and Gras (1991) and Ayers et al. (1991)
53 as evidence supporting a major role for marine biogenic reduced sulfur source in driving the CCN seasonal concentration
54 cycle. This CCN subset of the aerosol population has the ability to modify cloud physical and optical properties across a
55 substantial fraction of the relatively pristine Southern Ocean area, a potential climate impact first identified by Twomey (1974).

56 The likely significant role of marine biogenic sources providing precursors for secondary aerosol in the remote MBL has led
57 to suggestion of potential feedback mechanisms, particularly the CLAW hypothesis by Charlson et al. (1987). CLAW, named
58 after the author’s initials, proposes regulation of global temperature by DMS emission, through CCN-driven cloud albedo
59 feedback. Despite considerable development in understanding chemical processes and transport, as well as recent studies
60 extending earlier surface-based seasonal coherence studies to wider areas through satellite remote sensing (e.g. Gabric et al.,
61 2002, Vallina et al., 2006), the relatively limited progress in validation of the CLAW hypothesis as summarised, for example

62 by Ayers and Cainey (2007) and referred papers, illustrates the extreme complexity of processes controlling particle number
63 population in the remote MBL. Quinn and Bates (2011) go further, arguing that the relatively simplistic feedback mechanism
64 via DMS emission as represented in the CLAW hypothesis probably does not exist.

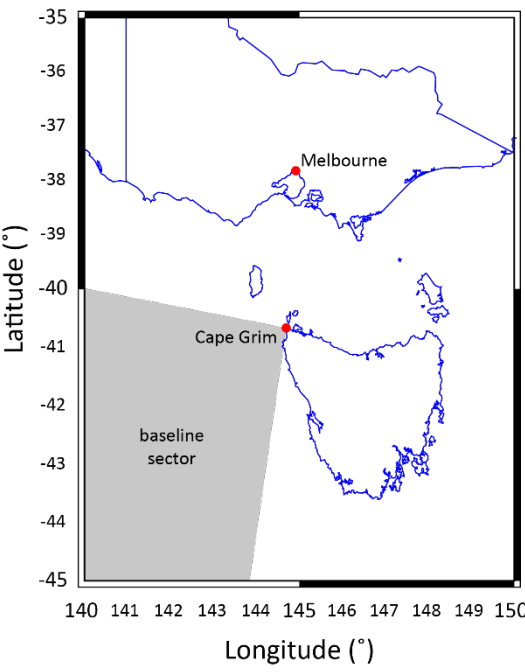
65 The overall response of natural production mechanisms in this region to climate change and even increasing anthropogenic
66 sources is still relatively uncertain and contributes to the overall uncertainty in future climate prediction due to indirect aerosol
67 forcing as illustrated in successive IPCC reports, recently by Boucher et al. (2013). The purpose of the present work is to
68 examine, or re-examine some characteristic features in the MBL aerosol at the relatively pristine site of Cape Grim, that should
69 provide a useful challenge and resource for the continually developing numerical models addressing these uncertainties.

70 **2 Methods -site description and instruments**

71 The Cape Grim baseline atmospheric program is the principal Australian contribution to the WMO Global Atmosphere Watch,
72 with an observatory located at the northwest tip of Tasmania (40° 41' S, 144° 41' E). Situated on a cliff and 94 m above sea
73 level the location maximises observation of Southern Ocean air that has had minimal recent anthropogenic impact. Air sampled
74 in the “Baseline” sector (190° – 280°) typically traverses several thousand kilometres of Southern Ocean since previous land
75 contact. The location of Cape Grim and the Baseline wind sector are shown in Fig. 1.

76 Measurement of airborne particles at Cape Grim commenced in the mid 1970s and generally sampling has followed what are
77 now WMO GAW Aerosol program recommendations (WMO 2003). N3 is effectively the total particle concentration and
78 concentrations reported here were determined using a TSI Ultrafine Condensation Particle Counter (CPC). N11 was
79 determined using TSI 3760 and TSI 3010 CPCs, CCN concentration for particles active at various supersaturations, but
80 primarily at 0.5% supersaturation, were determined using an automated static thermal gradient cloud chamber (Gras 1995).
81 Calibration of the CCN counter utilised a CPC (TSI 3760 / TSI 3010) and monodisperse particles of ammonium sulfate or
82 sodium chloride. The Koehler equation and van't Hoff factor approach were used to compute solute activity, as reported by
83 Low (1969). Size distribution data were obtained using an ASASP-X laser single particle size spectrometer, calibrated using
84 polystyrene latex spheres and corrected for refractive index to $m=1.473-0i$. A TSI 3790 mobility analyser with CPC (TSI 3010)
85 was also used to measure size distribution. Volatility measurements were made using a high temperature quartz tube furnace
86 with the CCN and CPC counters. Other reported measurements include Cape Grim methane sulfonic acid (MSA) and sea-
87 salt, from PM10 high-volume filter samples dimethyl sulfide (DMS), as described by Ayers and Gillett (2000) and estimates
88 of surface UV radiation based on satellite and ground based observations. UV radiation data, as midday erythral irradiance
89 (250-400 nm, weighted) were obtained from the NASA TOMS satellite record for the region upwind of Cape Grim (40-45°S
90 110-130°E) available from <http://macuv.gsfc.nasa.gov/>. UV irradiance values were also computed using ozone column data
91 for Melbourne (38°S 145°E), determined by the Australian Bureau of Meteorology using the empirical model of Allaart et

92 al. (2004). For the available overlap of the two UV irradiance records the correlation coefficient of monthly values is $r^2=0.99$
93 ($n=290$).



94
95 **Fig. 1. Map of south-eastern Australia and Tasmania, showing the location of the Cape Grim Baseline Air Pollution Station and**
96 **clean air “Baseline” sector.**

97 **3 Short term processes and CCN concentration**

98 The Southern Ocean region upwind of Cape Grim comprises part of the “roaring forties” which are strong westerly winds that
99 generally occur between 40 and 50 degrees south. It is a term persisting from the days of sailing ships and has a well-earned
100 and enduring reputation for strong and persistent winds. For 1999-2006, for example, median wind speed for the Baseline
101 maritime sector was 10.7 ms^{-1} , the 5th percentile was 3.4 ms^{-1} , and the 95th percentile 19.1 ms^{-1} . Most primary particle sources
102 over the Southern Ocean can be expected to be wind-dependent such as spray and bubble processes, and at higher wind speeds
103 windshear or spindrift; in addition wind is important for dispersal.

104
105 The background particle size distribution in the MBL at Cape Grim is typically tri-modal and the two modes of most obvious
106 interest from a CCN perspective for summer are shown in Fig. 2a. Baseline conditions (local wind direction $190\text{--}280^\circ$) were
107 selected using ambient radon concentration of less than 150 mBq m^{-3} ; this includes approximately 80% of Baseline sector

108 observations. Concentration data were derived using an ASASP-X size spectrometer for December, January February 1990-
 109 1995 and are plotted as median concentrations over 6 ms^{-1} wind bands.
 110 Cumulative concentrations for particles with diameters between $\sim 117 \text{ nm}$ - 350 nm , $D > 350 \text{ nm}$ and $D > 1000 \text{ nm}$ for the
 111 same data are shown in Fig. 2b.
 112
 113 Concentration in the coarse mode size range increases with wind speed (Figs. 2a and 2b); this is a widely reported phenomena
 114 resulting from bubble and spray mechanisms of wind generation of sea-salt particles for which there are a number of numerical
 115 parameterisations, see for example Gong (2003). Wind generated sea salt is normally the most abundant aerosol mass
 116 component over the Southern Ocean, with typical PM₁₀ sea-salt mass loadings at Cape Grim around $12 \mu\text{g m}^{-3}$. This coarse
 117 salt mode dominates the volume distribution throughout the year, although in number concentration the mode contribution is
 118 small; as shown, for example by Covert et al. (1998) the contribution to CCN_{0.5} in late spring 1995 was around 16%. The
 119 particle number concentration for the coarse mode was determined by fitting log-normal volume distribution functions for
 120 ASASP-X data in selected (6 ms^{-1}) wind bands for data collected during 1991-1994. For winter, combination of these observed
 121 representative size distributions with the more complete record of wind dependent concentrations for $D > 350 \text{ nm}$ yields an
 122 overall median number concentration of 26.6 cm^{-3} for the coarse mode. During the summer the coarse mode provides only a
 123 small fraction of particles in the CCN size range. Early work by Gras and Ayers (1983) using electron microscopy of individual
 124 particles, found that typically 1% of particles at 100 nm were clearly identifiable as sea-salt at Cape Grim in summer. While
 125 considerable work has been reported on understanding wind-dependent generation of sea salt, some aspects including the
 126 distribution of sea salt for sizes less than around 100 nm are still quite poorly characterised (Bigg 2007).
 127
 128 In contrast to the increase in particle concentration in the sea-salt dominated coarse mode, in summer the $115\text{-}350 \text{ nm}$ size
 129 range particle concentration decreases with increasing wind speed (Fig. 2b). This size range in the Southern Ocean MBL is
 130 part of a size mode centred at about 120 nm that is strongly associated with CCN. Although this mode is generally referred to
 131 as the accumulation mode, given its importance in cloud processing in the MBL it is identified here as the accumulation/CCN
 132 mode. Particles in this mode were shown to be volatile by Hoppel et al. (1986), who proposed an in-cloud growth mechanism
 133 involving aqueous-phase photochemical oxidation of gaseous precursors together with the physical processes of diffusion and
 134 coalescence.
 135 As shown in Figs. 2a and 3 the accumulation/CCN mode is strongest in summer and although it is also present in winter, it is
 136 often vestigial and difficult to separate from the coarse mode in single particle distributions.
 137 The evidence of negative wind speed dependence in the accumulation/CCN mode amplitude for current-hour wind-speed in
 138 summer is an interesting feature of this mode, as is the very sharp changeover from a positive relationship with wind speed in
 139 the coarse mode to the negative relationship in the accumulation/CCN mode, occurring at around 350 nm diameter at the mode
 140 intersection and within a narrow range of less than 50 nm .

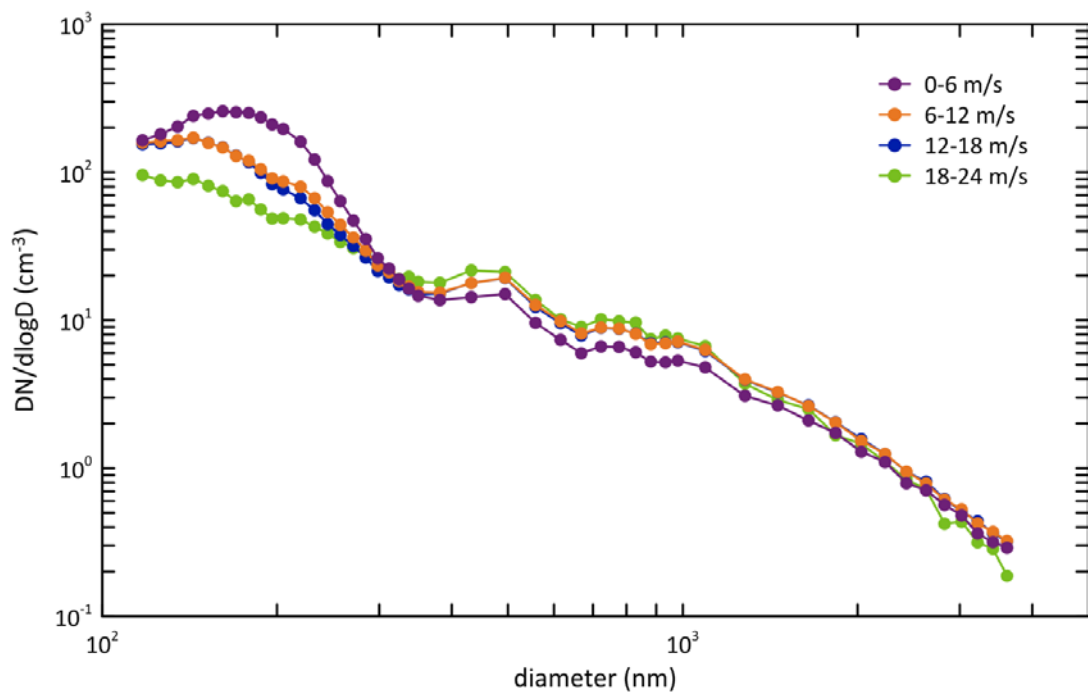


Fig. 2a. Summer clean MBL size distributions in 6 m s^{-1} wind bands, medians of hourly data

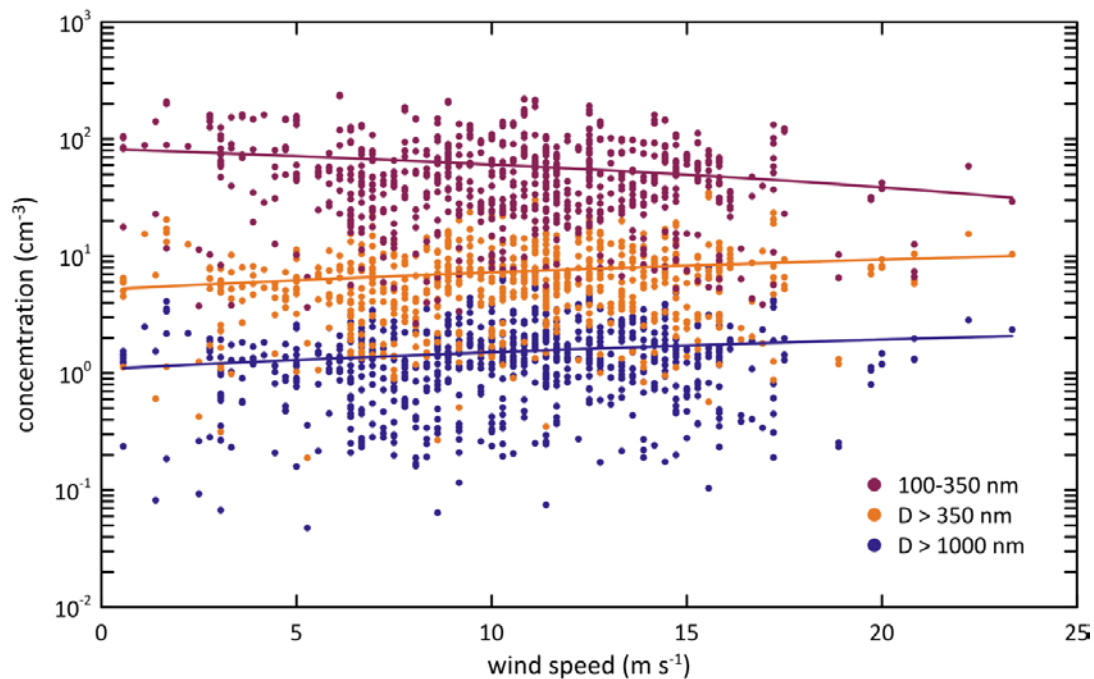
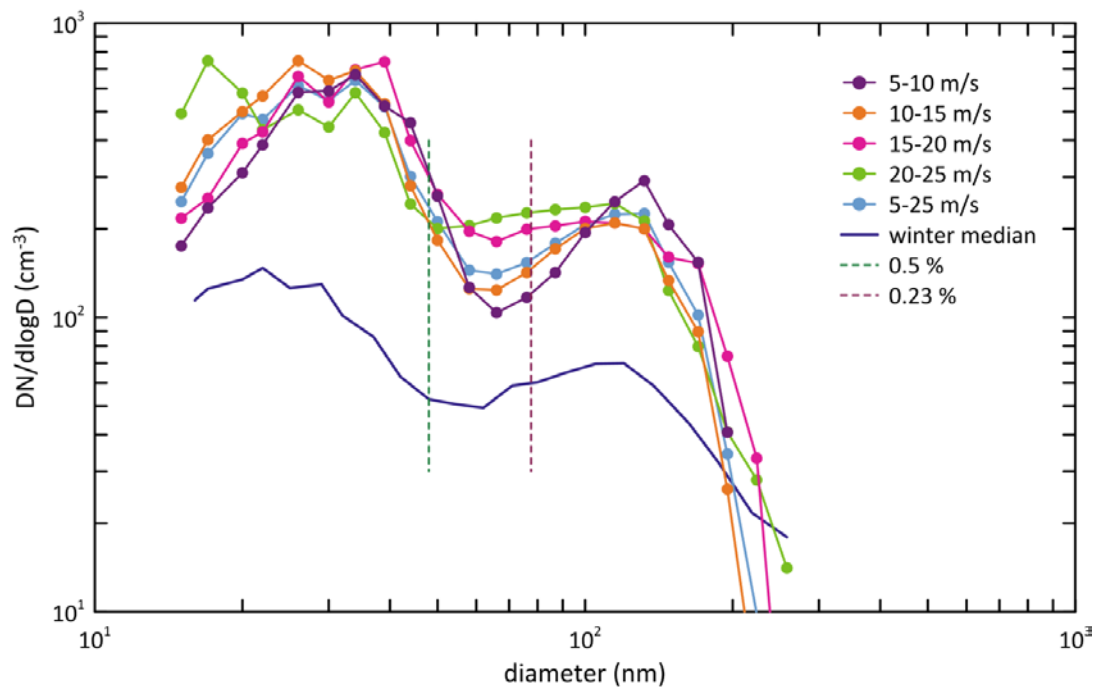


Fig. 2b. Cumulative concentration as a function of wind speed for accumulation/CCN mode (117 nm – 350 nm) and for $D > 350 \text{ nm}$ and $D > 1000 \text{ nm}$.



147
148 **Fig. 3. DMA derived size distribution including Aitken-accumulation/CCN mode gap as a function of wind speed.**

149 3.1 Wind strength and CCN concentration

150 A more extensive series of concentrations of CCN, N3 and N11, here covering the “Baseline” sector conditions for 1999-2006
151 gives more information on wind speed dependence in these integral measures, and allows some inferences on mode behaviour.
152 For summer, with selection of Baseline conditions using radon concentrations $< 150 \text{ mBeq m}^{-3}$, the CCN0.5 dependence on
153 wind speed overall is negative and represents a change for the median of about -14 cm^{-3} at 20 ms^{-1} (from 121 cm^{-3} at zero wind
154 speed), while additional restriction to wind speed greater than 7 ms^{-1} changes this dependence to positive overall and represents
155 $+9 \text{ cm}^{-3}$ at 20 ms^{-1} ; this is shown in Fig. 4.

156 Subtracting the coarse mode wind dependence determined from the ASASP size spectrometer results in much stronger negative
157 wind dependence for CCN0.5. This is predominantly due to the accumulation/CCN mode and now represents a change of
158 close to -60 cm^{-3} at 20 ms^{-1} for the median. Restriction to wind speeds greater than 7 ms^{-1} reduces this dependence slightly,
159 giving a change of around -51 cm^{-3} at 20 ms^{-1} .

160 Particle concentrations increase rapidly with decreasing wind speed for speeds less than around 7 ms^{-1} and when more relaxed
161 radon baseline criteria are applied, indicating the influence of local coastal effects and particularly recirculation of air that has
162 had recent land contact. Only minor improvement in rejection of potentially land-contaminated samples results from radon
163 selection threshold less than 150 mBeq m^{-3} , although added screening to exclude low wind speeds is preferable.

164

165 In winter for wind speed greater than 7 ms^{-1} , CCN_{0.5} concentration increases with increasing wind speed. Fig. 5 shows the
 166 population of CCN selected for radon concentration less than 150 mBeq m^{-3} and wind speed $> 7 \text{ ms}^{-1}$, and the change for 20
 167 ms^{-1} for the median's trend is around 25 cm^{-3} (from a reference level of $\sim 31 \text{ cm}^{-3}$ at zero wind speed). As in the case of summer,
 168 subtraction of the wind-dependence for the coarse mode results in a moderately strong negative trend for the
 169 accumulation/CCN mode component, representing a change of -12 cm^{-3} at 20 ms^{-1} .
 170 Figure 5 includes the wind-dependent concentration of CCN active at 0.6% supersaturation observed by Bigg et al. (1995)
 171 from ship-based measurements over the far Southern Ocean ($50\text{--}54^\circ\text{S}$) around mid-winter, under conditions where
 172 photochemical production should be minimal. The wind dependence of the concentration of coarse mode particles at Cape
 173 Grim, utilising fitted wind-dependent volume size distributions from data collected with an ASASP-X single particle size
 174 spectrometer during winters over 1991-1994 and as described earlier, is also given in Fig. 5. In addition, non-volatile aerosol
 175 concentrations determined in three 5 ms^{-1} wind bands, at Cape Grim over two weeks in different winters are shown. These
 176 volatility measurements showed no systematic difference between 350°C and 900°C , providing some evidence that the
 177 relationship observed by Bigg et al. (1995), the Cape Grim coarse mode and a significant proportion of CCN at 0.5%
 178 supersaturation at Cape Grim in winter, for high wind speeds, are composed of primary sea-salt.
 179 The expected principal removal mechanism in the CCN size range is nucleation scavenging, (Gras 2009), and dominance of
 180 this loss mechanism on a regional scale is supported by the statistical analysis by Vallina et al. (2006). Nucleation scavenging
 181 should be equally effective across both accumulation/CCN and coarse modes although removal in the coarse mode is masked
 182 by wind-related primary production; in addition some offset in the accumulation/CCN mode is likely from increased transfer
 183 of DMS at the ocean surface. Other microphysical loss processes include washout, "dry" deposition to the surface through
 184 increased spray generation with subsequent scavenging, and increased diffusion to large aerosol surface area, although none
 185 of these removal mechanisms readily explains the rapid reversal of wind dependence around 350 nm diameter. The negative
 186 wind dependence in the accumulation/CCN mode and reversal in dependence around 350 nm are consistent with competing
 187 processes to DMS oxidation modulating the strength of the accumulation/CCN mode. This includes heterogeneous reaction
 188 of SO_2 on sea-salt spray as suggested by Sievering et al. (1991), although the chemical mechanism leading to enhanced sulfate
 189 production on spray aerosol has been debated (Laskin et al. 2003, Keene et al. 2004, Sander et al. 2004, von Glasow 2006).
 190 Another possible mechanism is a sink for H_2SO_4 on super-micron salt aerosol (Yoon and Brimblecombe 2002). Both these
 191 mechanisms could potentially reduce the availability of reactive gases for in-cloud processing, and contribute to negative wind
 192 dependence of accumulation/CCN mode particle concentration.
 193 Over the Southern Ocean, increased wind speed is usually associated with more intense cyclonic systems, accompanied by
 194 increased convection, cloudiness and precipitation probably providing the major link between accumulation/CCN mode and
 195 wind speed. On a local scale at Cape Grim, monthly wind speed and rainfall data are only weakly positively correlated ($r^2 =$
 196 0.12 , Baseline) and the correlation for hourly data e.g. for summer using past 12h accumulated rainfall and current wind speed
 197 (excluding within 12 h of a front) is even weaker ($r^2 = 0.0006$). This is a weakness of fixed site observations which reveal only
 198 the immediate state of processes along a Lagrangian pathway taken by an air parcel.

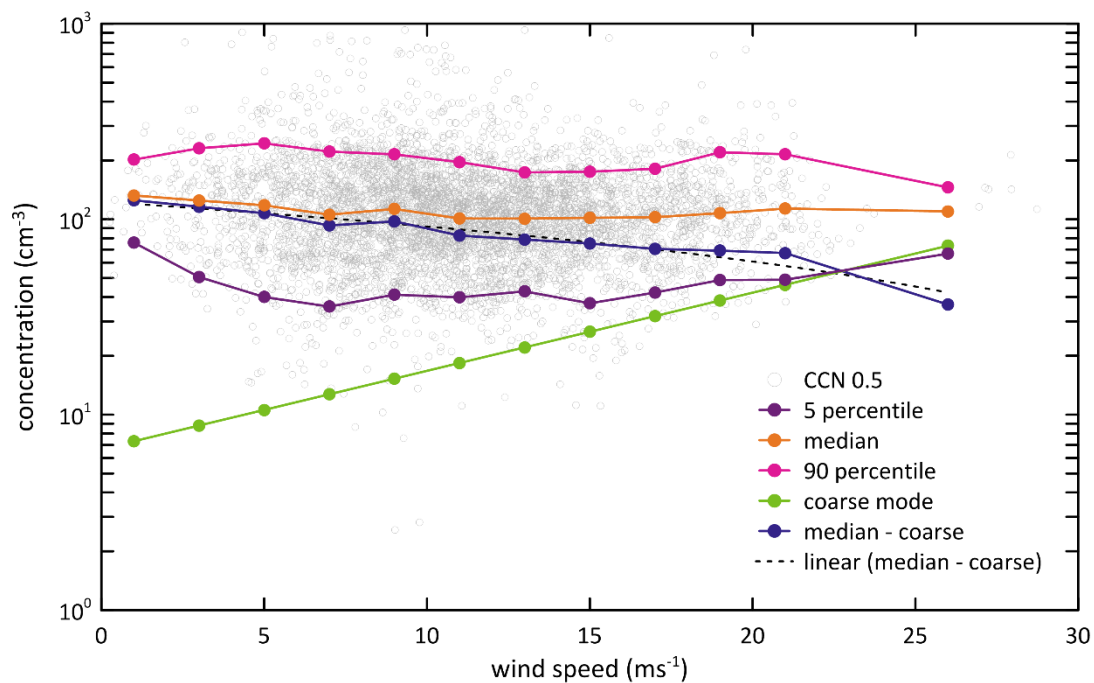


Fig. 4. CCN0.5 concentration as a function of wind speed, summer, radon $< 150 \text{ mBeq m}^{-3}$.

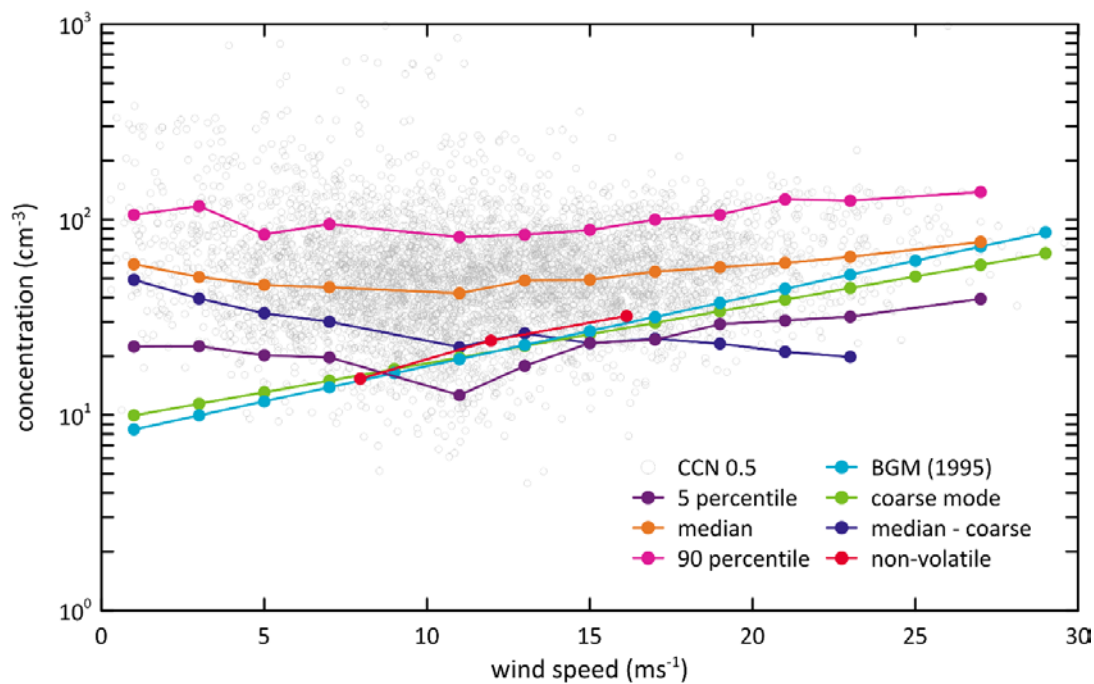


Fig. 5. CCN0.5 concentration as a function of wind speed, winter, radon $< 150 \text{ mBeq m}^{-3}$. BGM (1995) is the CCN active at 0.6% supersaturation observed by Bigg et al. (1995).

205 Mobility-derived particle size distributions for Cape Grim summers show some evidence of increased convection associated
 206 with stronger winds (Fig 3). As suggested by Hoppel et al. (1986), the dip between the Aitken and cloud-processed modes are
 207 a measure of the smallest particles that nucleate cloud droplets for this environment. For the cases considered (i.e. 2126
 208 summer distributions), the minimum between the modes decreases from around 66 nm at 5-10 ms^{-1} to around 50 nm at 20-25
 209 ms^{-1} and the spread in particle sizes broadens to smaller sizes such that over all conditions the mode diameter is around 115
 210 nm while for 20-25 ms^{-1} concentrations are relatively flat with a broad mode between 60 nm and 130 nm. These values also
 211 illustrate the typical supersaturation levels for this environment; assuming an ammonium bisulphate/MSA mixture, the typical
 212 supersaturation experienced (calculated using Kohler theory) would be somewhat greater than 0.15%, since mode size
 213 represents typical particles exiting clouds. The mode of particles passing through the cloud process extends down to 50–66
 214 nm (0.45% - 0.3% supersaturation) depending on environmental conditions (indicated by wind strength). Under the more
 215 convective conditions a much greater fraction of CCN active at 0.5% would be classified as being in the upper end of the
 216 Aitken mode. The instrumental value of 0.5% supersaturation used as the primary measure of CCN at Cape Grim provides a
 217 conservative lower size bound that captures the accumulation/CCN mode under most environmental conditions, albeit at the
 218 expense of including a small and variable fraction of Aitken mode particles.

219 Particle concentration integrated across the full size spectrum does not show strong wind dependence, for example the
 220 relationship between N11 and wind speed in summer (for data selected with $ws > 5 \text{ ms}^{-1}$ and $\text{radon} < 150 \text{ mBeq m}^{-3}$) is weakly
 221 positive, representing an overall increase of around 54 cm^{-3} at 20 ms^{-1} or 11% (from a concentration of 482 cm^{-3} not related to
 222 wind speed). In winter with the same selection criteria the trend is around +56% against a reference of 104 cm^{-3} , although this
 223 represents a similar concentration increase, in this case 58 cm^{-3} at 20 ms^{-1} . These trends are close to those expected from the
 224 coarse mode and subtraction of the parameterised coarse mode leaves the overall trend across the Aitken and accumulation
 225 modes relatively small, at -6 cm^{-3} in summer and $+20 \text{ cm}^{-3}$ in winter (for a wind strength change of 20 ms^{-1}). Using the
 226 difference in N11 and CCN0.5 concentrations and the same wind speed and radon selection criteria as a measure of the
 227 (integrated) Aitken mode concentration indicates a positive dependence in summer of $+40 \text{ cm}^{-3}$ at 20 ms^{-1} , relative to 364 cm^{-3}
 228 3 not related to wind speed change, and in winter a similar concentration increase but greater fractional change of $+26 \text{ cm}^{-3}$ at
 229 20 ms^{-1} (relative to 67 cm^{-3} not related to wind speed change) for the Aitken mode.

230 This shift in balance between production and removal for the Aitken mode with increasing wind speed could potentially include
 231 wind-generated sub-50 nm diameter primary sea-salt particles (e.g. Clarke et al., 2006), although it is also entirely consistent
 232 with enhanced free troposphere-MBL exchange from a dominant free-tropospheric particle number source, following the
 233 mechanisms summarised for example by Raes et al. (2000).

234 The concentration of nanoparticles defined here as N3-N11 also increases with wind speed, for data with the same wind speed
 235 and radon selection criteria described above. For summer the concentration increase for a 20 ms^{-1} wind speed increase is
 236 around $+8 \text{ cm}^{-3}$ and in winter 12 cm^{-3} .

237 While overall the integrated particle number in the MBL over the clean Southern Ocean is only weakly dependent on wind
 238 speed, the wind dependence of the different modes that comprise the full aerosol spectrum is complex. For CCN the balance

239 between a positive wind dependence in the coarse mode and negative dependence in the accumulation/CCN mode leads to a
240 relatively flat wind dependence in summer and moderately strong positive wind dependence in winter. The change-over in
241 wind dependence of these two modes occurs in a very small size range at the mode intersection, indicative of a different
242 balance of production and removal in the coarse and accumulation/CCN modes.

243 **4 CCN seasonal variation and covariances**

244 The second aspect of MBL particle behaviour considered here is a re-examination of seasonal covariances and implications
245 for factors influencing particle concentrations on a seasonal time scale. Use of extended time series of a seasonally-varying
246 species at one site allows accumulation of data over many cycles and filtering of non-seasonal factors, suppressing both shorter
247 term weather noise and longer term inter-annual variation. Figure 6, for example, shows the seasonal variation in N3 and CCN
248 (0.5%) at Cape Grim together with surface level solar UV irradiance derived from reported total ozone for Melbourne, for the
249 period 1978-2006. Data plotted are monthly medians and CCN (0.5%) concentrations have been offset in amplitude in the
250 plot, to provide approximate alignment with the N3 cycle over the autumn-winter period.

251 Fig. 6 illustrates the different behaviour of the three variables over summer (Dec-Feb). Whereas the UV variation is
252 approximately sinusoidal, N3 tends to flatten or limit and CCN concentration has a clear, cusp-like summer peak. Over the
253 winter part of the year (Jun-Aug) CCN concentrations are relatively constant. This presentation of annual cycles for the three
254 parameters, with approximate synchronisation in late autumn-winter also highlights marked differences in phase between UV,
255 N3 and CCN, with CCN concentrations lagging N3 by around 1-2 months leading into the summer maximum. These seasonal
256 cycles in general are relatively robust although for CCN in a few summers including 1997, 2004 and 2005, there was no
257 significant January peak.

258 Expressed as bivariate relationships with UV, N3 and CCN concentrations both show some seasonal hysteresis (different
259 response going from summer to winter to that for winter to summer) although for these aggregated seasonal data the variance
260 in N3 explained just by seasonal UV changes is high, around 97% (for a quadratic fit), and for CCN, UV change explains
261 around 87% of the seasonal monthly variance (Fig. 7). This makes no assumptions about the processes between UV irradiation
262 and particle number concentration, although clearly the hysteresis can be expected to be related to these processes. The
263 potential role of marine ecology in providing a source of reduced sulfur species that can transfer into the MBL atmosphere and
264 then be oxidised and condensed to particles has been very widely reported, along with possible feedback mechanisms, for
265 example summarised by Vogt and Liss (2009). Although a minor species by mass, aerosol-bound MSA, an oxidation product
266 of DMS should represent a potentially useful near-specific proxy for this biogenic source and MBL mass production.
267 The seasonal cycles of monthly median CCN and MSA, as shown in Fig. 8 share many significant features, particularly
268 relatively constant autumn-winter concentrations and the sharp summer maximum.

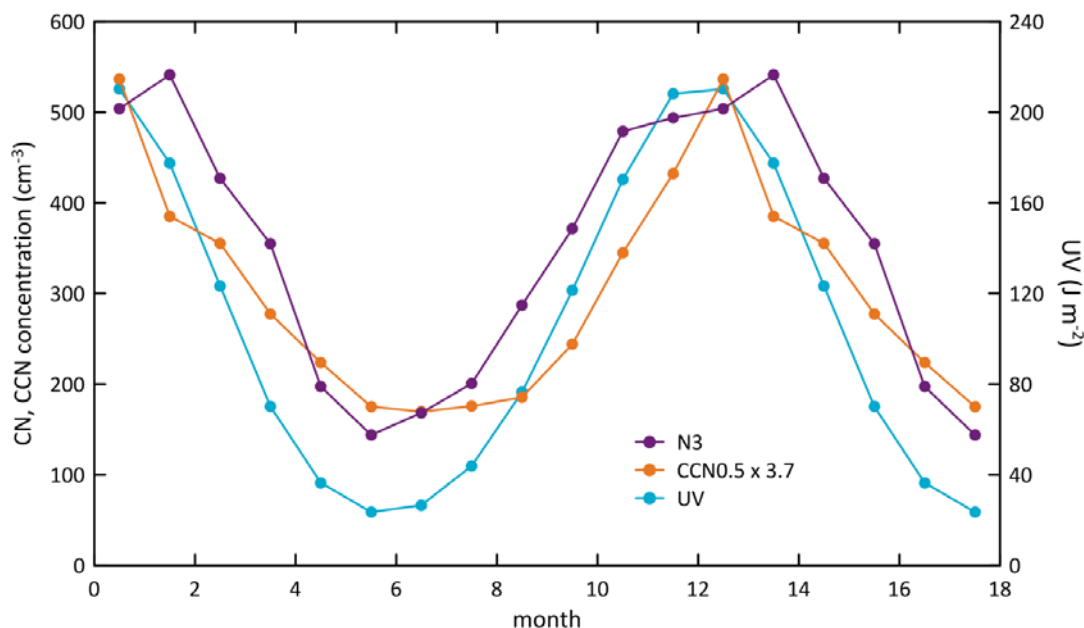


Fig. 6. Seasonal variation in N3(1978-2005)and CCN0.5(1981-2006) with radon <150 mBeq m⁻³, and UV(1978- 2005). N3 & CCN are monthly medians with 12 months data plotted as 18 months, summer is months 1,2,12,(13,14). CCN concentrations are scaled (x 3.7) to give a similar plotted amplitude range to N3.

Using MSA as independent variable, the non-linear relationship for N3 shown in Fig. 9 explains a similar variance in the seasonal cycle with UV as independent variable ($r^2=0.97$); the very small amount of change of N3 as MSA increases during the summer half-year (Oct-Mar) illustrates a near independence of N3 (Aitken mode) and MSA concentrations in this season). The level of variance explained in the CCN seasonal cycle using MSA as independent variable rises to 96%, a worthwhile improvement from the 87% explained by UV alone (Fig. 7). MSA effectively collapses the hysteresis that was evident using the UV/photochemistry proxy and this level of correlation with the CCN annual cycle is consistent with the hypothesised role of marine biogenic sources in driving the seasonal pulse in MBL CCN number concentration.

As illustrated by Fig. 8, the very characteristic flat winter and sharply peaked summer underlying seasonal cycles for MSA and CCN do not directly track the UV annual cycle, although both are very well described by the product of current month DMS and UV irradiance. Correlation of the monthly MSA concentrations with DMS x UV gives $r^2=0.97$, and correlation of CCN with DMS x UV $r^2=0.96$. UV here evidently represents a simple but reasonable proxy for photochemical oxidation of DMS. Strong correlation was reported between ocean upper mixed layer DMS concentration and UV dose by Toole and Siegel (2004), and more pertinently across the global ocean surface by Vallina and Simó (2007). At Cape Grim the seasonal pattern of atmospheric DMS does not directly track that of UV and regression between current month values for DMS with UV explains only around 85% of the seasonal variance. As illustrated by Fig. 10 for MSA, the DMS cycle reaction products are much better described by the product of current month and previous month UV ($r^2=0.95$) indicative of two dominant radiation-

291 limited processes with a time difference somewhere around one month. Vallina et al. (2006) consider a possible lag of between
292 a few days to two weeks between chlorophyll levels and an effect on CCN. Their analysis produced slightly lower correlations
293 between their CCN proxy and the product of chlorophyll and OH with a two week lag of their atmospheric parameters, although
294 their lag is referenced to chlorophyll levels and not irradiance.

295 The close seasonal relationship evident between MSA and the product of current and previous month UV irradiance, as shown
296 for MSA monthly median data in Fig. 10, and the very similar relationship for CCN and irradiance afford a simple
297 approximation to the dominant underlying seasonal driver, albeit stripped of all other potential modulating factors, including
298 biotic and physical processes.

299 If current month UV is used as a proxy for all photochemical production of CCN_{0.5}, regression of CCN on UV produces a
300 non-photochemical offset of around 31 cm^3 (30.7 ± 7.0 , ± 1 standard error), Fig.7. The implied photochemically-derived
301 CCN component (from this regression) represents 74% of the observed Cape Grim summer median CCN concentration
302 whereas for winter the non-photochemical fraction (regression offset) dominates, contributing 65% of the observed median
303 CCN.

304 For the case where MSA is taken as a proxy for the more specific marine-biogenic photochemically-produced MBL aerosol
305 mass, regression with CCN_{0.5} (as in Fig. 9) gives a non-seasonal offset of around 48 cm^3 (48.7 ± 2.7). In this case the
306 seasonal secondary component, identified with marine biogenic sources represents 60% of the observed summer median CCN
307 concentration (for 1981-2006 monthly median data). In winter this marine biogenic component makes no significant
308 contribution to the median CCN concentration.

309 This compares reasonably well with fractions derived for the broader Southern Ocean by Vallina et al. (2006) using correlation
310 based on remotely sensed chlorophyll as an indicator of marine biogenic reactive precursor sources, modelled OH and an
311 aerosol optical depth (AOD) fraction proxy for CCN. These authors estimate a marine biogenic fraction of 80% of the proxy
312 CCN in summer falling to 35% in winter, which compares better with the fractions derived above for the in-situ CCN data
313 using the UV/photochemical proxy, than those using MSA, a more direct proxy of marine biogenic secondary aerosol. There
314 are several possible explanations for differences in the two approaches including the comparison of surface observations with
315 column integrals. Also the remotely sensed proxy CCN involves conversion of AOD to fine fraction aerosol volume to CCN
316 number concentration; the accuracy of the physical representation of the parameterisations and of the overall proxy in
317 representing the in-situ CCN population across the broader ocean environment have had extremely limited validation (e.g see
318 Gasso and Hegg 2003, Hegg and Kaufman 1998).

319

320

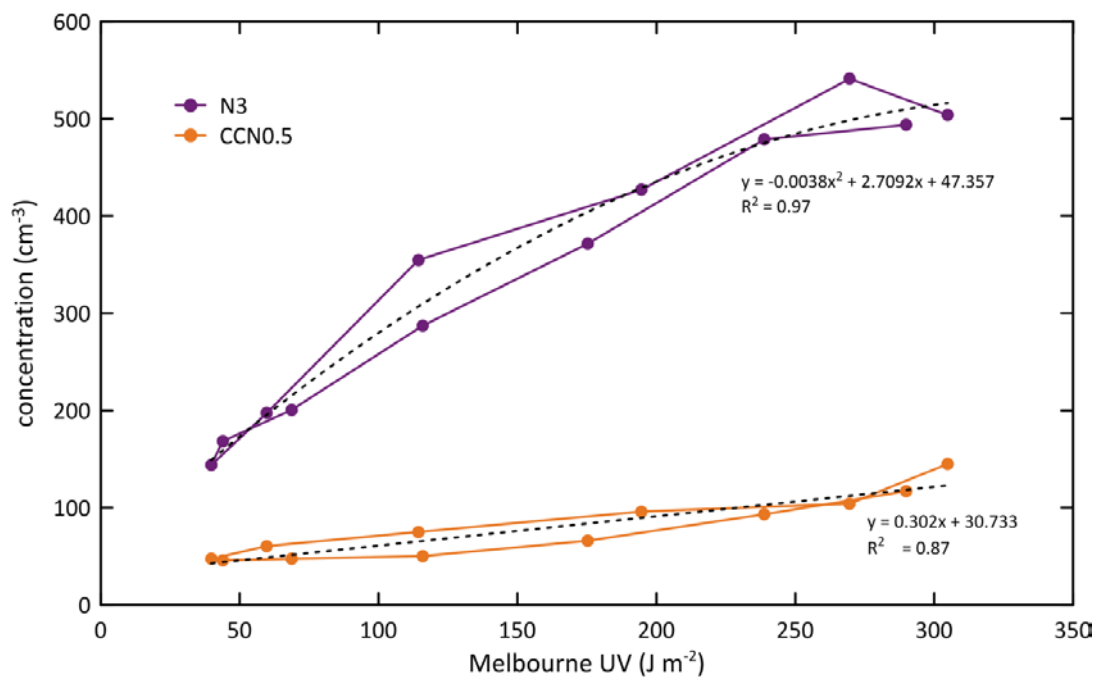


Fig. 7. Melbourne UV 1976-2008, median CCN with radon<150 mBeq m⁻³ 1981-2006, and median CN

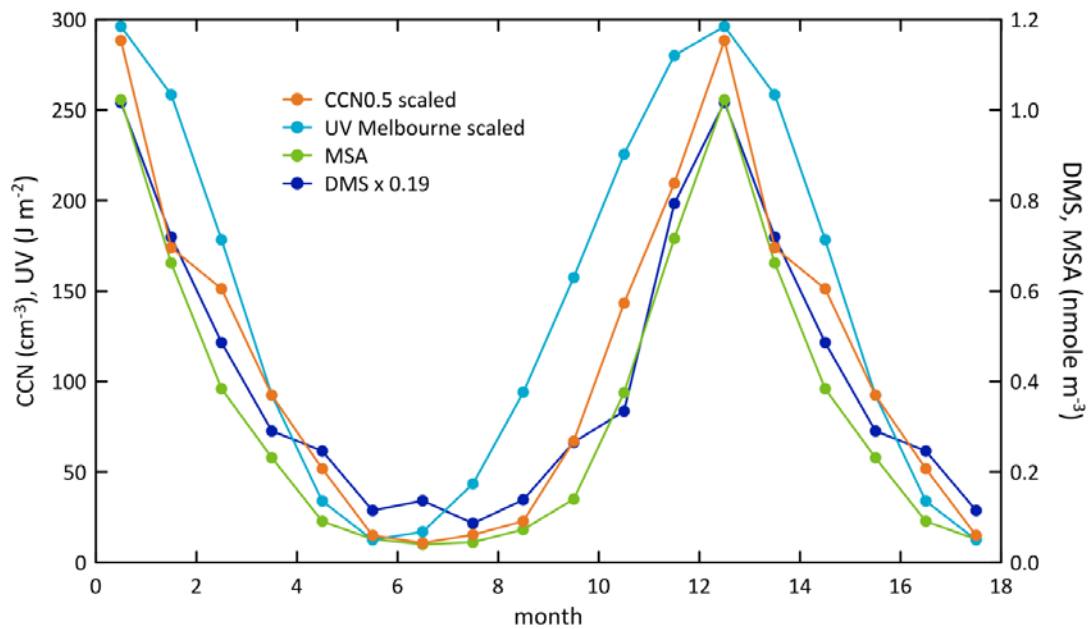
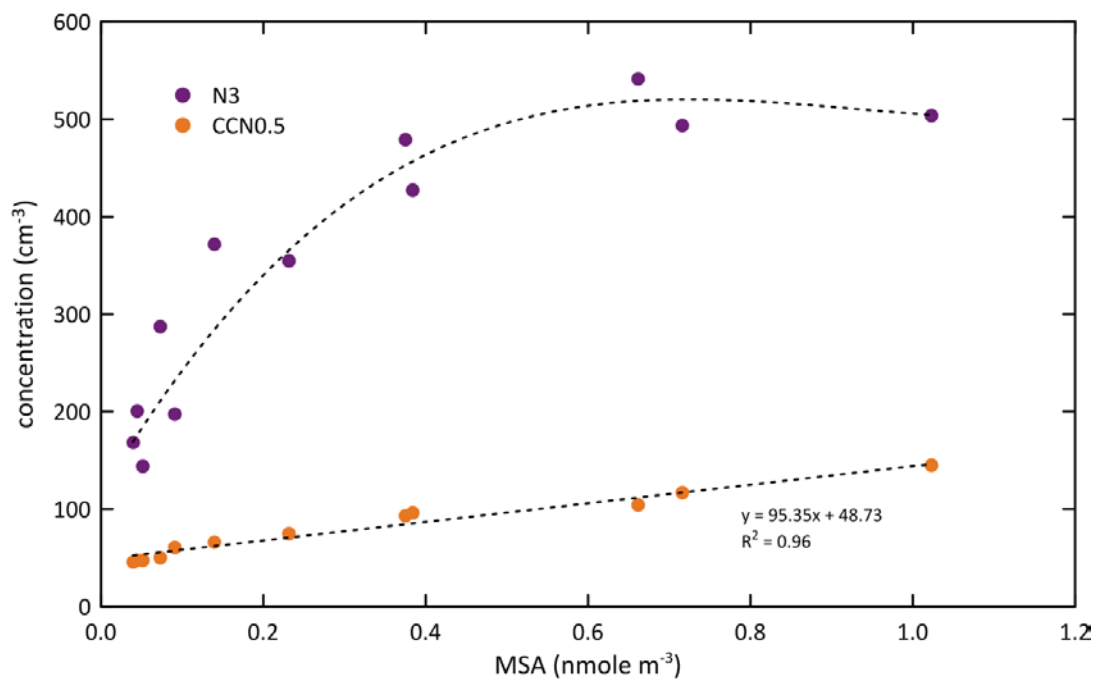
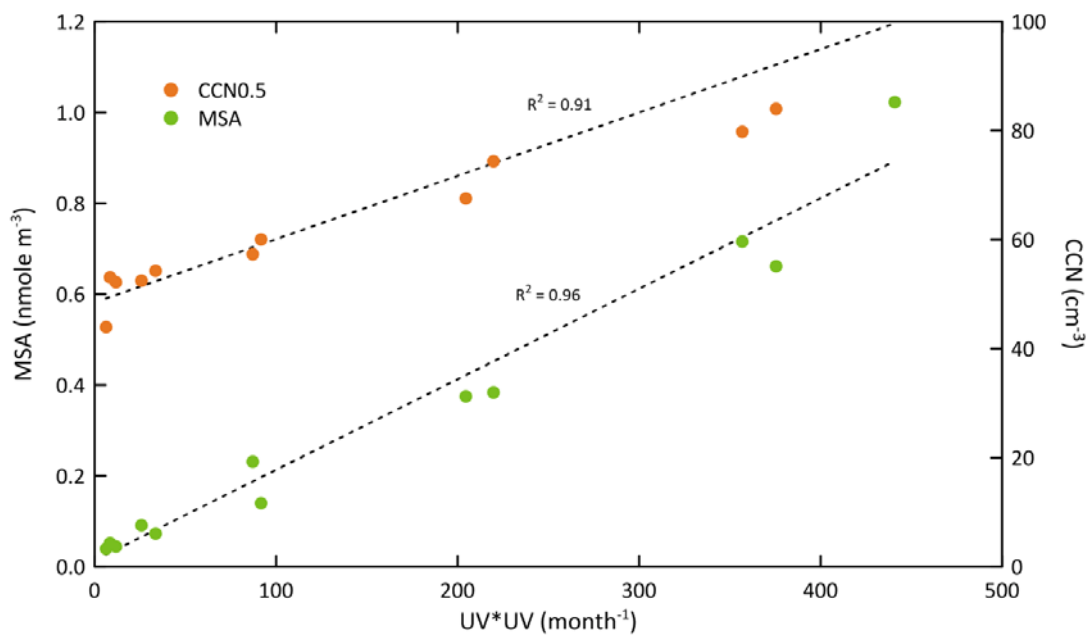


Fig. 8. CCN and MSA (ccn median -1981-2006, [scaled], MSA median 1985-2007, UV Melbourne 1976-2008)



328
329
330 **Fig. 9. Bivariate N3 (1978-2005), CCN 1981-2006 with radon < 150 mBeq m⁻³ MSA 1985-2007 (monthly medians)**



332
333
334 **Fig. 10. MSA and CCN0.5 dependence on UV * UV-1 month**

336 The offset in CCN_{0.5} of approximately 31 cm^{-3} at zero UV levels (Fig. 7) represents a non-photochemical contribution that
 337 should include any water-active primary particles including wind generated sea-salt and any primary organic/biogenic material
 338 not seasonally linked to the summer pulse. The CCN concentration - wind speed relationship, for CCN at 0.6% determined
 339 over the far Southern Ocean (50-54°S), in mid-winter by Bigg et al. (1995) and the winter coarse mode concentration at Cape
 340 Grim determined from size spectrometer measurements at Cape Grim as a function of wind speed, discussed above, suggest a
 341 typical coarse wind-generated concentration around $20\text{-}27 \text{ cm}^{-3}$. Whilst the major component in this fraction is likely to be
 342 sea salt, it may also contain some primary biogenic aerosol material (PBAM) of marine origin, such as exopolymer gels,
 343 organisms, marine gels, insoluble organics and fragments; together these comprise a potentially important, but grossly
 344 understudied aerosol component (e.g. Jaenicke 2005, Leck and Bigg 2008). In one measurement campaign at Cape Grim in
 345 summer 2006 Bigg (2007) found that 9% of particles with $D > 200 \text{ nm}$, and possibly up to 30% of particles with $80\text{-}200 \text{ nm}$
 346 contained PBAM inclusions thus were potentially of importance for CCN activity. However, neither the actual impact of
 347 PBAM on CCN activity nor the contribution at smaller sizes is certain. Also since the only measurements are from in summer,
 348 it is impossible to gauge the relationship between this class of particle and UV radiation; they might comprise a small subgroup
 349 of the 60% of CCN already attributed to secondary marine biogenic sources, or alternatively be considered as part of the non-
 350 photochemical primary particle group.

351 Regression of N₃ and current month UV gives a non-UV (non-photochemical) offset of 47 cm^{-3} , assuming no correlation
 352 between primary sources and UV (Fig. 7). This includes the seasonally-invariant population of particles that are also active
 353 as CCN at 0.5% (around 31 cm^{-3}), and a smaller population of particles that could be water active but are smaller than the CCN
 354 activation diameter.

355 **5 CCN mode/source contributions and composition**

356 Some broad estimate of the various sources contributing to the CCN population is possible using regression procedures with
 357 the previously indicated proxies; in this section both CCN active at 0.5% and the population of CCN active at 0.23% are
 358 considered. Whilst these populations substantially overlap giving a measure of redundancy, the CCN_{0.23} population excludes
 359 a fraction of the smaller particles present in CCN_{0.5} and thus presents a slightly simpler particle microphysics picture.

360 For CCN_{0.23} the MSA proxy plus a seasonally-invariant component explains 96% of the variance in the CCN_{0.23} seasonal
 361 cycle. Wind speed and hence coarse mode salt has a very minor seasonal cycle (amplitude range around $\pm 2\%$) with a weak
 362 peak around late winter-early spring, not in phase with MSA) and is treated as part of the invariant component; this can be
 363 removed either before or after regression with similar results. The contributions to CCN_{0.23} concentration from back-
 364 substitution of the regression coefficients are shown in Fig. 11, for an analysis utilising MSA, a coarse mode based on the
 365 observed wind speed relationship and in this case one “other”, so far unspecified component.

366 While correlation between the underlying CCN and MSA annual cycles has been known for some time (e.g. Ayers and Gas
 367 1991) and has giving significant insights into the MBL’s annual sulfur cycle, it is significant that the MSA-like component,

368 taken here as a proxy for marine biogenic sources, only dominates the Southern Ocean CCN population for the 3 summer
369 months; the CCN0.23 component with the largest average contribution overall (from this analysis) is the “other” component
370 (representing 46% of CCN0.23 annually, or $\sim 28 \text{ cm}^{-3}$); the wind-generated coarse mode varies in importance from 2nd to 3rd
371 most important depending on the time of year. This wind-generated coarse mode is 2nd most important from March-October
372 (autumn through to mid-spring), when the seasonal pulse in biogenic activity leads to dominance by the MSA proxy, or marine
373 biogenic source.

374 For CCN0.5 multiple linear regression with two major proxies, MSA as described above with CCN0.23 for MBL sources and
375 an additional proxy for Aitken mode particles (N3) explains 97% of the annual cycle monthly variance. This produces a
376 seasonally-invariant component of around 38 cm^{-3} and, as for CCN0.23, this is further partitioned into two components
377 “coarse” and “other” in Fig. 12. In this case the MSA proxy represents the largest single CCN0.5 component for 5 months of
378 the year but it still only provides greater than 50% of the CCN for three months (Fig. 12). From this analysis annual average
379 MSA, coarse (sea salt) and “other” proxies explain approximately equal annually-averaged contributions to CCN0.5 (26%,
380 28.5% and 27%).

381 Some contribution to CCN0.5 and at greater supersaturations, is expected from larger particles in the Aitken mode, as shown
382 by Covert et al. (1998) and here also from the observed size distributions. The present analysis gives average summer and
383 winter CCN0.5 concentrations of 22 cm^{-3} and 7 cm^{-3} due to the Aitken mode compared with the corresponding mobility-
384 derived size distribution estimates of 38 and 5 cm^{-3} .

385 The overall broad estimates for the number concentrations of CCN0.23 and CCN0.5 based on the present analyses and wind-
386 dependence of coarse mode particles is summarised in Table 1. While the MSA-like fraction is interpreted here as arising
387 through secondary production of mass in the MBL particularly nssSO₄ and MSA it could include organic material emitted and
388 photo-reacted with a seasonal cycle similar to that of MSA production. Likewise, for the Aitken mode contribution based on
389 the N3 proxy, composition is more likely to reflect nucleation and growth in the free troposphere (Bigg et al. 1984, Raes 1995)
390 and will potentially include some long-range transported precursors.

391 A lack of convincing mass-composition “closure” for the CCN mode (100-300 nm) in the Southern Ocean MBL aerosol
392 remains an issue, with data on size-dependent composition for this mode relatively sparse, particularly data on either soluble
393 or insoluble organics; there is also a strong bias towards composition data relating to the spring-summer period and little for
394 winter.

395

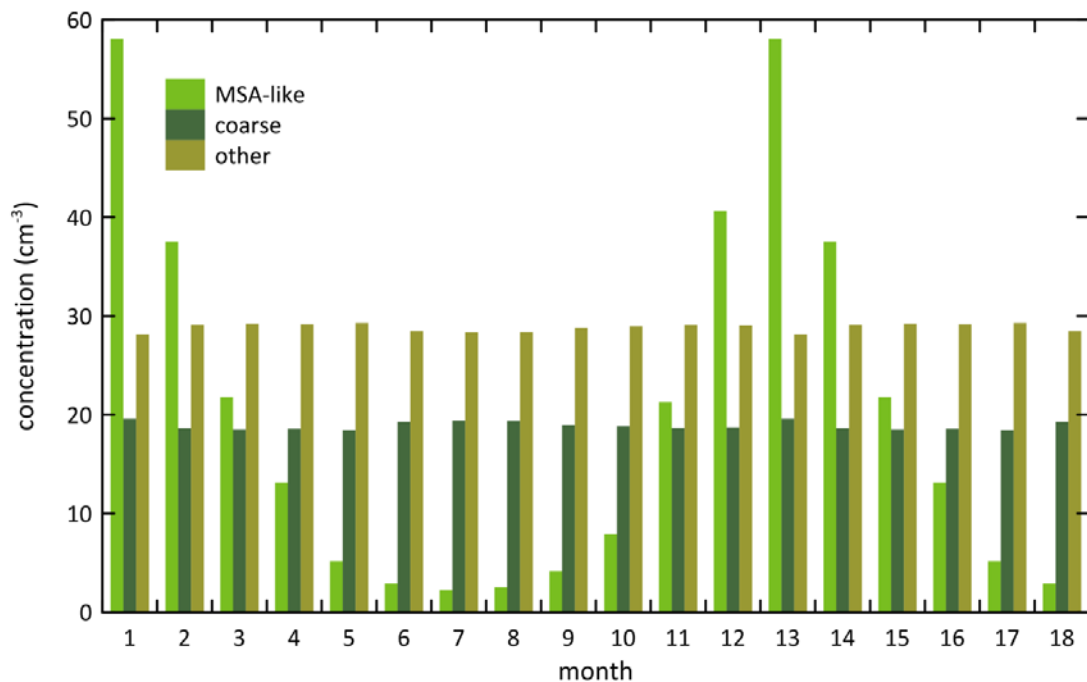


Fig. 11. CCN.23 population based on MSA-CCN.23 regression with seasonally-invariant factor separated into a wind-generated “coarse” contribution and one “other” invariant factor.

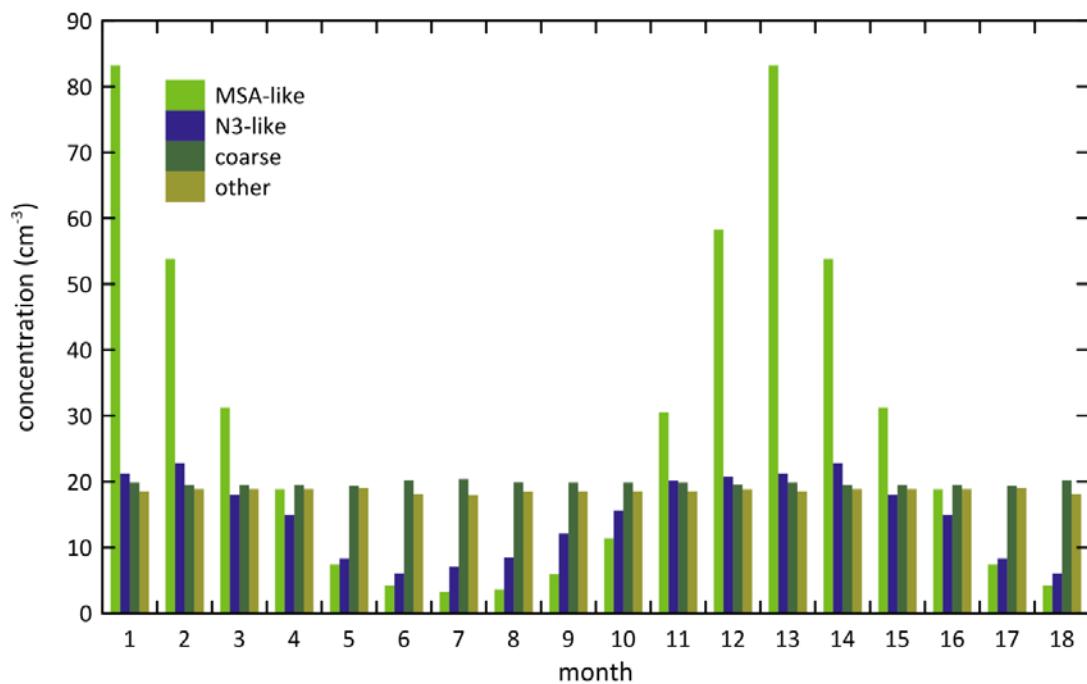


Fig. 12. Multiple linear regression for CCN at 0.5% supersaturation as a function of 4 parameters

401 **Table 1 Fractional contribution to CCN at 0.23% and 0.5% supersaturation from current analyses.**

		Aitken-like	MSA-like	coarse (SS)	other (LRT)
CCN0.23	summer		48	21	31
	winter		5	38.5	56.5
	annual		23	31	46
CCN0.5	summer	17.5	51.5	16	15
	winter	14.5	7.5	41	37
	annual	18.5	26	28.5	27

402

403 Single particle analyses for this size range by Gras and Ayers (1983) showed dominance of sulfate-containing particles during
404 summer at Cape Grim (external mixture with 95% sulfate-containing, internally 11% non-sulfate by volume, ~1%
405 undetermined and the residual sea-salt). This method utilised a barium thin film test for sulfate and the barium salt of MSA is
406 soluble, so should not appear in the sulfate fraction. The method was not specifically tested for MSA interference so cannot
407 be ruled out, but this suggests the non-sulfate fraction was most likely MSA. In summer at Cape Grim impactor collections
408 by Caine (1997) for this size range indicate MSA close to 20% of sulfate mass loading.
409 During ACE-1 in spring-summer (Nov-Dec) Middlebrook et al. (1998) identified an approximately 10% organic fraction in a
410 size range that includes the CCN mode ($D > 160$ nm) but only in conjunction with sea-salt particles, and no pure organic
411 particles. MOUDI samples from Huebert et al. (1998) show major non-sea-salt soluble species of sulfate, ammonium and
412 MSA. For the CCN-size range the missing mass fraction was 10-47% of the measured mass but uncertainty was an equivalent
413 magnitude. Indirect determinations for accumulation mode particles from ACE-1 (Nov-Dec) using an H-TDMA, Berg et al.
414 (1998), Covert et al. (1998), are consistent with sulfate/bisulfate and a small, $< 10\%$, insoluble content. A few isolated
415 measurements in February 2006 by Fletcher et al. (2007), using a VH-TDMA system are also consistent with sulfate/bisulfate
416 as the major hygroscopic fraction but suggested variability in composition and an insoluble content ranging from 0-60%.
417 Caine (1997) also determined soluble ion composition mass size distributions for the size range 100-300 nm from 1993-1994
418 using a MOUDI sampler and showed the predominance of sulfate and ammonium in the non-sea salt fraction over all seasons
419 and MSA reaching about 20% of sulfate mass loading in summer (a similar pattern to bulk sampling) and around 2% in winter.
420 Increased awareness of the magnitude, variability and potential role of an organic fraction in the MBL, as both water soluble
421 and insoluble fractions (e.g. O'Dowd et al. 2004, O'Dowd and Leeuw 2007) questions the predominantly inorganic-based
422 view. Northern Hemisphere observations have shown significant organic fractions associated with biologically active episodes
423 and this further highlights a lack of corresponding in-situ observations near highly biologically active regions in the southern
424 oceans. As discussed previously this applies also to marine primary biological aerosol, the actual role of which for CCN
425 concentration remains.

426 5.1 Seasonally-invariant CCN fraction

427 The component of the seasonally-invariant fraction named “other” in the CCN regression analyses clearly has no directly
428 identifiable information on the chemical composition of the CCN mode. Impactor analyses by Cainey (1997) have soluble-
429 ion-mass modes identifiable with both the accumulation/CCN mode and Aitken modes which comprise at least non-sea-salt
430 sulfate, ammonium, MSA and oxalate. For winter these size dependent data for $100 < D < 300\text{nm}$, which captures the mass
431 mode dominating the CCN population yield a total sulfate concentration of 24 ng m^{-3} and non-sea-salt sulfate 16 ng m^{-3} ;
432 including other soluble ions (ammonium, MSA, oxalate) gives a known mode non-sea-salt ion mass of 25.4 ng m^{-3} .

433 Multiple regression of the non-sea-salt sulfate annual cycle from multi-decadal high-volume sampler bulk samples at Cape
434 Grim, also using MSA and N3 as proxies similarly explains around 97% of the seasonal variance in non-sea-salt sulfate and
435 gives a seasonally-invariant component of 22 ng m^{-3} (see Fig 13). Normalising the non-sea-salt ion mass from the MOUDI
436 distributions based on the non-sea-salt sulfate mode mass (16 ng m^{-3}) gives an expected mean (winter) accumulation/CCN
437 mode mass of 35 ng m^{-3} for the measured non-sea-salt ion fraction. Based on the residual MSA concentration in this winter
438 CCN mode, only a small fraction ($\sim 2\%$) of this summed accumulation/CCN mode mass would be attributable to the MSA
439 source.

440 The multiple linear regressions for CCN0.23 and CCN0.5 provide two estimates of the non-seasonal component in the
441 accumulation/CCN mode number concentration. After removing the measured wind-speed based coarse mode concentration,
442 which itself has only very weak seasonal dependence and averages around 20 cm^{-3} for CCN0.5 and 19 cm^{-3} for CCN0.23, the
443 winter mean residual or “other” fraction is 28 cm^{-3} based on CCN0.23 and 18 cm^{-3} based on CCN0.5. Of these two estimates
444 CCN0.5 is considered the more accurate, given an increasing uncertainty in measurement with decreasing supersaturation in
445 the static CCN counter, and lower sample frequency for CCN0.23 in the Cape Grim CCN program.

446 These CCN number concentrations are readily converted to an equivalent mass concentration for any given particle density,
447 using size distributions determined at Cape Grim by mobility analysis. The average summer size distribution with a density
448 of 1.77 g cm^{-3} (corresponding to ammonium sulfate/bisulfate) gives corresponding mass loadings of 37 ng m^{-3} for CCN0.5 and
449 62 ng m^{-3} for CCN0.23, which compare well with the median winter size distribution yields mode mass loadings of 34 ng m^{-3}
450 for CCN0.5 based and 65 ng m^{-3} for CCN0.23 based. For this approximate mass closure the combined data suggest that the
451 majority, and possibly all of the otherwise unexplained or non-sea salt component in the seasonally-invariant factor in the CCN
452 concentration multiple linear regression analyses is comprised primarily of ammonium sulfate/bisulfate and minor light
453 organics; this implies disconnection from both the seasonal pulse in marine biogenic activity and UV annual cycle, instead
454 being likely associated with long range transport (LRT), potentially including an anthropogenic contribution.

455 Estimates by Korhonen et al. (2008) of the contribution of continental sources to CCN0.23 for $30\text{--}45^\circ\text{S}$, using the chemical
456 transport model GLOMAP, range from $\sim 20\text{ cm}^{-3}$ in winter to 25 cm^{-3} in summer; these values are consistent with interpreting
457 the constant minus coarse component estimates from multiple regression as LRT. The regressions then imply $\sim 28\text{ cm}^{-3}$ and
458 29 cm^{-3} (Winter, Summer) for CCN0.23 and $\sim 18\text{ cm}^{-3}$ and 19 cm^{-3} (Winter, Summer) for CCN0.5 as possible LRT. Clearly

the regression analysis cannot distinguish continental precursor contributions that add to MBL sources if these react in phase with MBL sources. In the free troposphere for example these are likely to contribute to the Aitken mode number, and mass generation, but otherwise lose their identity. The use of a detailed model with specific sources turned off, illustrates well the potential non-linear contribution of different sources, whereas multiple linear regression by definition identifies potential factors contributing to CCN number variance. A similar issue applies for example to fine primary sea spray which may contribute to some of the kernels of CCN but not necessarily control the evolution of particles into CCN. Recent determination of sulfur budgets for the dry, subsiding tropical marine boundary layer by Simpson et al. (2014) point to analogous contributions to non-sea-salt sulfate from DMS production and free tropospheric entrainment (including LRT). In their study DMS appears responsible for only around one third of observed non-sea-salt sulfate, the remainder being attributed to entrainment from the free troposphere.

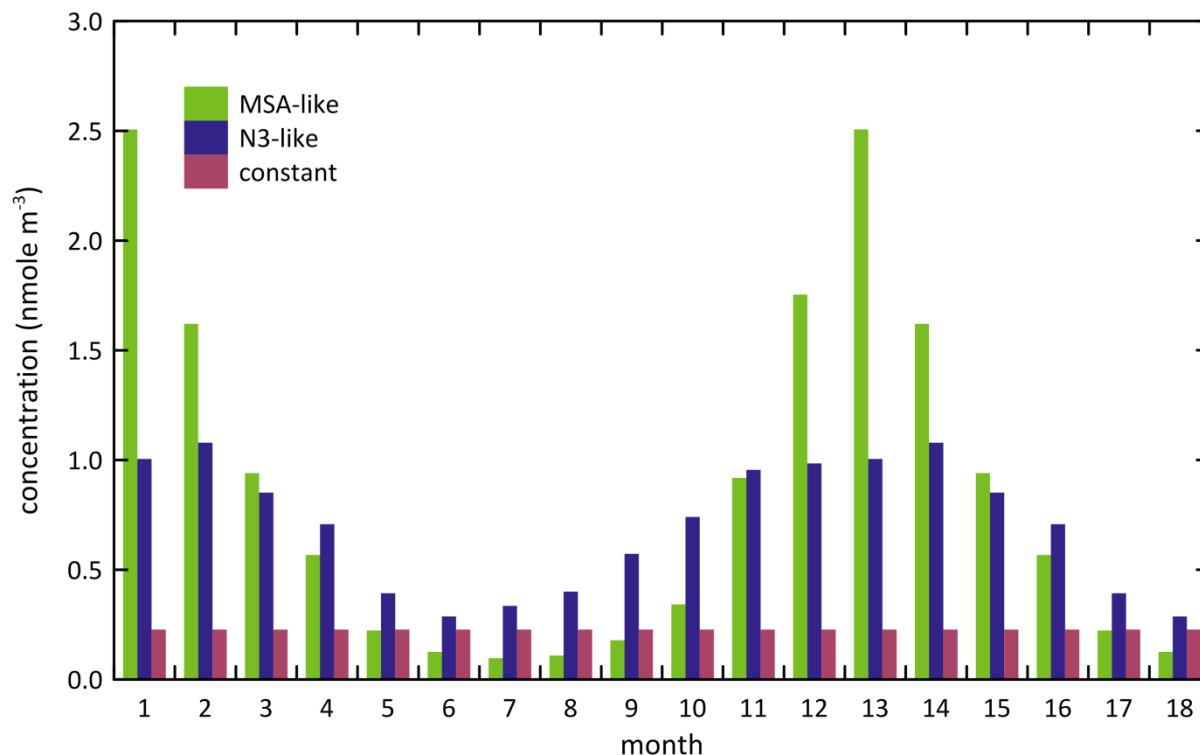


Fig. 13. Multiple linear regression for non-sea-salt sulfate as a function of 3 parameters (MSA, N3, constant)

6 Conclusions

The purpose of the present work has been to examine data on CCN concentration together with other aspects of the long term MBL aerosol measurements at Cape Grim that should provide a useful challenge to developing regional or global numerical models. These analyses show that while the marine biological source of reduced sulfur appears to dominate CCN concentration over summer, the previous strong focus on understanding sulfur cycling in the Southern Ocean MBL has somewhat

overshadowed the importance of other CCN components taken on a full annual basis. The observations show that wind-generated coarse mode sea-salt is an important CCN component year round and from autumn through to mid spring for example is second most important, contributing around 36% (for CCN_{0.23}). For greater supersaturations, as expected in more convective cyclonic systems and their associated fronts, Aitken mode particles become increasingly important as CCN. One characteristic feature of this component is a different seasonal cycle to CCN number overall, which has a sharp summer concentration peak. Previous regression analyses of CCN concentration have consistently indicated a non-seasonal component, part of which can clearly be attributed to wind generated sea-salt and the remainder includes features that can be attributed to long range transported material. Significant contribution to the CCN population by particles from the three major size modes with seasonal change in importance of these contributions leads to a complex wind dependence. Capturing the balance due to the combination of different mode behaviours, as shown in the observations, is clearly a challenge to be met by numerical simulations hoping to predict changes in CCN population in a changing climate.

Author contributions

J L Gras designed and led the measurement program until 2011, carried out data analysis and wrote the manuscript, M Keywood led the measurement programs since 2011 and contributed to writing the manuscript.

Data availability

Data are available from the authors; hourly median concentrations (CCN and CN₁₁) from 2012-2015 are available in the World Data Centre for Aerosols.

Acknowledgements

Continued support for this program through CGBAPS research funds and the personal effort of numerous Cape Grim support staff maintaining equipment over the program lifetime is gratefully acknowledged. Ozone data determined by the Australian Bureau of Meteorology were obtained from the World Ozone and Ultraviolet Radiation Data Centre (WOUDC) operated by Environment Canada, Toronto, Ontario, Canada under the auspices of the World Meteorological Organization: http://www.woudc.org/data_e.html. Radon data were provided by Wlodek Zharovski and Stewart Whittlestone from ANSTO. Paul Selleck is thanked for carrying out aerosol analyses and Nada Derek is thanked for producing the figures in the manuscript.

References

Aman, A. A. and Bman, B. B.: The test article, J. Sci. Res., 12, 135–147, doi:10.1234/56789, 2015.

503 Aman, A. A., Cman, C., and Bman, B. B.: More test articles, *J. Adv. Res.*, 35, 13–28, doi:10.2345/67890, 2014.

504 Allaart, M., van Weele, M., Fortuin, P., and Kelder, H.: An empirical model to predict the UV-index based on solar zenith
 505 angles and total ozone, *Meteorological Applications*, 11, 59–65, 10.1017/s1350482703001130, 2004.

506 Ayers, G. P., and Gras, J. L.: Seasonal relationship between cloud condensation nuclei and aerosol methanesulfonate on marine
 507 air, *Nature*, 353, 834–835, 1991.

508 Ayers, G. P., Ivey, J. P., and Gillett, R. W.: Coherence between seasonal cycles of dimethyl sulfide, methanesulfonate and
 509 sulfate in marine air, *Nature*, 349, 404–406, 10.1038/349404a0, 1991.

510 Ayers, G. P., and Gillett, R. W.: DMS and its oxidation products in the remote marine atmosphere: implications for climate
 511 and atmospheric chemistry, *Journal of Sea Research*, 43, 275–286, [http://dx.doi.org/10.1016/S1385-1101\(00\)00022-8](http://dx.doi.org/10.1016/S1385-1101(00)00022-8), 2000.

512 Ayers, G. P., and Cainey, J. M.: The CLAW hypothesis: a review of the major developments, *Environmental Chemistry*, 4,
 513 366–374, 10.1071/en07080, 2007.

514 Berg, O. H., Swietlicki, E., and Krejci, R.: Hygroscopic growth of aerosol particles in the marine boundary layer over the
 515 Pacific and Southern Oceans during the First Aerosol Characterization Experiment (ACE 1), *Journal of Geophysical Research-*
 516 *Atmospheres*, 103, 16535–16545, 10.1029/97jd02851, 1998.

517 Bigg, E. K., Gras, J. L., and Evans, C.: Origin of Aitken particles in remote regions of the Southern Hemisphere, *Journal of*
 518 *Atmospheric Chemistry*, 1, 203–214, 10.1007/bf00053841, 1984.

519 Bigg, E. K., Gras, J. L., and Mossop, D. J. C.: Wind-produced submicron particles in the marine boundary layer, *Atmospheric*
 520 *Research*, 36, 55–68, 1995.

521 Bigg, E. K.: Sources, nature and influence on climate of marine airborne particles, *Environmental Chemistry*, 4, 155–161,
 522 10.1071/en07001, 2007.

523 Boucher, O., Randall, D., Artaxo, P., Bretherton, C., Feingold, G., Forster, P., Kerminen, V.-M., Kondo, Y., Liao, H.,
 524 Lohmann, U., Rasch, P., Satheesh, S. K., Sherwood, S., Stevens, B., and Zhang, X. Y.: Clouds and aerosols. In *Climate Change*
 525 *2013: The Physical Science Basis. Contribution of Working Group I to the Fifth Assessment Report of the Intergovernmental*
 526 *Panel on Climate Change*. T.F. Stocker, D. Qin, G.-K. Plattner, M. Tignor, S.K. Allen, J. Doschung, A. Nauels, Y. Xia, V.
 527 Bex, and P.M. Midgley, Eds. Cambridge University Press, 571–657, doi:10.1017/CBO9781107415324.016., 2013.

528 Cainey, J. M.: The atmospheric sulfur cycle in the remote southern ocean environment, PhD Thesis, Monash University,
 529 Melbourne, Australia, 320 pp., 1997.

530 Charlson, R. J., Lovelock, J. E., Andreae, M. O., and Warren, S. G.: Oceanic phytoplankton, atmospheric sulfur, cloud albedo
 531 and climate, *Nature*, 326, 655–661, 1987.

532 Clarke, A. D., Owens, S. R., and Zhou, J. C.: An ultrafine sea-salt flux from breaking waves: Implications for cloud
 533 condensation nuclei in the remote marine atmosphere, *Journal of Geophysical Research-Atmospheres*, 111, D06202
 534 10.1029/2005jd006565, 2006.

535 Covert, D. S., Gras, J. L., Wiedensohler, A., and Stratmann, F.: Comparison of directly measured CCN with CCN modeled
 536 from the number-size distribution in the marine boundary layer during ACE 1 at Cape Grim, Tasmania, *Journal of Geophysical*
 537 *Research-Atmospheres*, 103, 16597-16608, 10.1029/98jd01093, 1998.
 538 Fletcher, C. A., Johnson, G. R., Ristovski, Z. D., and Harvey, M.: Hygroscopic and volatile properties of marine aerosol
 539 observed at Cape Grim during the P2P campaign, *Environmental Chemistry*, 4, 162-171, 10.1071/en07011, 2007.
 540 Gabric, A. J., Cropp, R., Ayers, G. P., McTainsh, G., and Braddock, R.: Coupling between cycles of phytoplankton biomass
 541 and aerosol optical depth as derived from SeaWiFS time series in the Subantarctic Southern Ocean, *Geophysical Research*
 542 *Letters*, 29, 1112
 543 10.1029/2001gl013545, 2002.
 544 Gasso, S., and Hegg, D. A.: On the retrieval of columnar aerosol mass and CCN concentration by MODIS, *Journal of*
 545 *Geophysical Research-Atmospheres*, 108, 4010
 546 10.1029/2002jd002382, 2003.
 547 Gong, S. L.: A parameterization of sea-salt aerosol source function for sub- and super-micron particles, *Global Biogeochemical*
 548 *Cycles*, 17, 109710.1029/2003gb002079, 2003.
 549 Gras, J. L., and Ayers, G. P.: Marine aerosol at southern mid-latitudes, *Journal of Geophysical Research: Oceans*, 88, 10661-
 550 10666, 10.1029/JC088iC15p10661, 1983.
 551 Gras, J. L.: CN, CCN and particle size in the Southern Ocean air at Cape Grim, *Atmospheric Research*, 35, 233-251, 1995.
 552 Gras, J. L.: Postfrontal nanoparticles at Cape Grim: impact on cloud nuclei concentrations, *Environmental Chemistry*, 6, 515-
 553 523, 10.1071/en09076, 2009.
 554 Hegg, D. A., and Kaufman, Y. J.: Measurements of the relationship between submicron aerosol number and volume
 555 concentration, *Journal of Geophysical Research-Atmospheres*, 103, 5671-5678, 10.1029/97jd03652, 1998.
 556 Hoppel, W. A., Frick, G. M., and Larson, R. E.: Effect of nonprecipitating clouds on the aerosol size distribution in the marine
 557 boundary layer, *Geophysical Research Letters*, 13, 125-128, 10.1029/GL013i002p00125, 1986.
 558 Huebert, B. J., Howell, S. G., Zhuang, L., Heath, J. A., Litchy, M. R., Wylie, D. J., Kreidler-Moss, J. L., Coppel, S., and
 559 Pfeiffer, J. E.: Filter and impactor measurements of anions and cations during the First Aerosol Characterization Experiment
 560 (ACE 1), *Journal of Geophysical Research-Atmospheres*, 103, 16493-16509, 10.1029/98jd00770, 1998.
 561 Jaenicke, R.: Abundance of cellular material and proteins in the atmosphere, *Science*, 308, 73-73, 10.1126/science.1106335,
 562 2005.
 563 Keene, W. C., and Pszenny, A. A. P.: Comment on "Reactions at interfaces as a source of sulfate formation in sea-salt particles"
 564 (I), *Science*, 303, 2004.
 565 Korhonen, H., Carslaw, K. S., Spracklen, D. V., Mann, G. W., and Woodhouse, M. T.: Influence of oceanic dimethyl sulfide
 566 emissions on cloud condensation nuclei concentrations and seasonality over the remote Southern Hemisphere oceans: A global
 567 model study, *Journal of Geophysical Research-Atmospheres*, 113, 10.1029/2007jd009718, 2008.

568 Laskin, A., Gaspar, D. J., Wang, W. H., Hunt, S. W., Cowin, J. P., Colson, S. D., and Finlayson-Pitts, B. J.: Reactions at
 569 interfaces as a source of sulfate formation in sea-salt particles, *Science*, 301, 340-344, 10.1126/science.1085374, 2003.
 570 Leck, C., and Bigg, E. K.: Comparison of sources and nature of the tropical aerosol with the summer high Arctic aerosol,
 571 *Tellus Series B-Chemical and Physical Meteorology*, 60, 118-126, 10.1111/j.1600-0889.2007.00315.x, 2008.
 572 Lee, Y. H., Adams, P. J., and Shindell, D. T.: Evaluation of the global aerosol microphysical Model E2-TOMAS model against
 573 satellite and ground-based observations, *Geoscientific Model Development*, 8, 631-667, 10.5194/gmd-8-631-2015, 2015.
 574 Low, R. D. H.: A generalised equation for solution effect in droplet growth, *Journal of the Atmospheric Sciences*, 26, 608-&,
 575 10.1175/1520-0469(1969)026<0608:agefts>2.0.co;2, 1969.
 576 Mann, G. W., Carslaw, K. S., Spracklen, D. V., Ridley, D. A., Manktelow, P. T., Chipperfield, M. P., Pickering, S. J., and
 577 Johnson, C. E.: Description and evaluation of GLOMAP-mode: a modal global aerosol microphysics model for the UKCA
 578 composition-climate model, *Geoscientific Model Development*, 3, 519-551, 10.5194/gmd-3-519-2010, 2010.
 579 Middlebrook, A. M., Murphy, D. M., and Thomson, D. S.: Observations of organic material in individual marine particles at
 580 Cape Grim during the First Aerosol Characterization Experiment (ACE 1), *Journal of Geophysical Research-Atmospheres*,
 581 103, 16475-16483, 10.1029/97jd03719, 1998.
 582 O'Dowd, C. D., Facchini, M. C., Cavalli, F., Ceburnis, D., Mircea, M., Decesari, S., Fuzzi, S., Yoon, Y. J., and Putaud, J. P.:
 583 Biogenically driven organic contribution to marine aerosol, *Nature*, 431, 676-680, 10.1038/nature02959, 2004.
 584 O'Dowd, C. D., Yoon, Y. J., Junkerman, W., Aalto, P., Kulmala, M., Lihavainen, H., and Viisanen, Y.: Airborne measurements
 585 of nucleation mode particles I: coastal nucleation and growth rates, *Atmospheric Chemistry and Physics*, 7, 1491-1501, 2007.
 586 Pierce, J. R., and Adams, P. J.: Global evaluation of CCN formation by direct emission of sea salt and growth of ultrafine sea
 587 salt, *Journal of Geophysical Research-Atmospheres*, 111, D06203
 588 10.1029/2005jd006186, 2006.
 589 Quinn, P. K., and Bates, T. S.: The case against climate regulation via oceanic phytoplankton sulphur emissions, *Nature*, 480,
 590 51-56, 10.1038/nature10580, 2011.
 591 Raes, F.: Entrainment of free tropospheric aerosols as a regulating mechanism for cloud condensation nuclei in the remote
 592 marine boundary layer, *Journal of Geophysical Research-Atmospheres*, 100, 2893-2903, 10.1029/94jd02832, 1995.
 593 Raes, F., Dingenen, R. V., Vignati, E., Wilson, J., Putaud, J.-P., Seinfeld, J. H., and Adams, P.: Formation and cycling of
 594 aerosols in the global troposphere, *Atmospheric Environment*, 34, 4215-4240, [http://dx.doi.org/10.1016/S1352-](http://dx.doi.org/10.1016/S1352-2310(00)00239-9)
 595 2310(00)00239-9, 2000.
 596 Sander, R., Crutzen, P. J., and von Glasow, R.: Comment on "Reactions at Interfaces As a Source of Sulfate Formation in Sea-
 597 Salt Particles" (II), *Science*, 303, 628c-628c, 10.1126/science.1090971, 2004.
 598 Sievering, H., Boatman, J., Galloway, J., Keene, W., Kim, Y., Luria, M., and Ray, J.: Heterogeneous sulfur conversion in sea-
 599 salt aerosol-particles- The role of aerosol water content and size distribution, *Atmospheric Environment Part a-General Topics*,
 600 25, 1479-1487, 10.1016/0960-1686(91)90007-t, 1991.

601 Simpson, R. M. C., Howell, S. G., Blomquist, B. W., Clarke, A. D., and Huebert, B. J.: Dimethyl sulfide: Less important than
 602 long-range transport as a source of sulfate to the remote tropical Pacific marine boundary layer, *Journal of Geophysical*
 603 *Research-Atmospheres*, 119, 9142-9167, 10.1002/2014jd021643, 2014.
 604 Spracklen, D. V., Pringle, K. J., Carslaw, K. S., Chipperfield, M. P., and Mann, G. W.: A global off-line model of size-resolved
 605 aerosol microphysics: I. Model development and prediction of aerosol properties, *Atmospheric Chemistry and Physics*, 5,
 606 2227-2252, 2005.
 607 Toole, D. A., and Siegel, D. A.: Light-driven cycling of dimethylsulfide (DMS) in the Sargasso Sea: Closing the loop,
 608 *Geophysical Research Letters*, 31, L09308 10.1029/2004gl019581, 2004.
 609 Twomey, S.: POLLUTION AND PLANETARY ALBEDO, *Atmospheric Environment*, 8, 1251-1256, 10.1016/0004-
 610 6981(74)90004-3, 1974.
 611 Vallina, S. M., Simo, R., and Gasso, S.: What controls CCN seasonality in the Southern Ocean? A statistical analysis based
 612 on satellite-derived chlorophyll and CCN and model-estimated OH radical and rainfall, *Global Biogeochemical Cycles*, 20,
 613 Gb1014 10.1029/2005gb002597, 2006.
 614 Vallina, S. M., and Simo, R.: Strong relationship between DMS and the solar radiation dose over the global surface ocean,
 615 *Science*, 315, 506-508, 10.1126/science.1133680, 2007.
 616 Vogt, M., and Liss, P. S.: Dimethylsulfide and Climate, in: *Surface Ocean: Lower Atmosphere Processes*, Volume 187, edited
 617 by: Le Quere, C., and Saltzman, E. S., 197-232, 2009.
 618 von Glasow, R.: Importance of the surface reaction OH+Cl- on sea salt aerosol for the chemistry of the marine boundary layer
 619 - a model study, *Atmospheric Chemistry and Physics*, 6, 3571-3581, 2006.
 620 Wang, M. H., Penner, J. E., and Liu, X. H.: Coupled IMPACT aerosol and NCAR CAM3 model: Evaluation of predicted
 621 aerosol number and size distribution, *Journal of Geophysical Research-Atmospheres*, 114, D06302
 622 10.1029/2008jd010459, 2009.
 623 WMO: GAW report 153 WMO/GAW Aerosol Measurement procedures guidelines and recommendations, 2003.
 624 Yoon, Y. J., and Brimblecombe, P.: Modelling the contribution of sea salt and dimethyl sulfide derived aerosol to marine CCN,
 625 *Atmos. Chem. Phys.*, 2, 17-30, 10.5194/acp-2-17-2002, 2002.
 626
 627